ELSEVIER

Biophysical Chemistry 82 (1999) 183–193

Biophysical Chemistry

www.elsevier.nl/locate/bpc

Accelerated diffusion of Na^+ in a hydrophobic region revealed by molecular dynamics simulations of a synthetic ion channel

Zhi Qi, Masahiro Sokabe*

Department of Physiology, Nagoya University School of Medicine, Tsurumai 65, 466-8550, Nagoya, Japan

Received 15 September 1999; accepted 15 September 1999

Abstract

To get insight into the significance of the hydrophobic lining on the ion permeation, we performed molecular dynamics simulations on a Na^+ permeation through a de novo synthetic hydrophobic channel. Electrophysiological study has suggested that the channel is formed from a tail-to-tail associated dimer of a cyclic octa-peptide coupled with hydrophobic acyl chains. The acyl chains line the channel pore while the cyclic peptide forms the channel entrance [Z. Qi, M. Sokabe, K. Donowaki, H. Ishida, Biophys. J. 76 (1999) 631]. Molecular dynamics simulation of water in the channel indicated that the inferred structure is physically reasonable [Z. Qi, M. Sokabe, Biophys. Chem. 71 (1998) 35]. In the present study, the potential energy profile of the Na^+ and the energy contributions from each component of the system at different positions along the channel axis were calculated. An energy well instead of a peak is located at the central hydrophobic cavity of the channel, due to its ability of accommodating at least five water molecules to hydrate the ion. Interestingly, the ion diffuses much faster in the hydrophobic acyl chain region, particularly in the central hydrophobic cavity, than it does in the peptide ring region and even surprisingly faster than that in the bulk phase. These results provide a physical basis for an idea that the hydrophobic lining of the K^+ channel [D.A. Doyle, J.M. Cabral, R.A. Pfuetzner, A. Kuo, J.M. Gulbis, S.L. Cohen, B.T. Chait, R. MacKinnon, Science 280 (1998) 69] plays an active role to facilitate the ion permeation through the channel pore.

Keywords: Molecular dynamics (MD) simulation; Energetics; Ion permeation; Hydrophobic channel; Diffusion coefficient; K^+ channel

* Corresponding author. Tel.: +81-52-744-2051; fax: +81-52-744-2057.
E-mail address: msokabe@med.nagoya-u.ac.jp (M. Sokabe)

0301-4622/99/$ - see front matter
PII: S0301-4622(99)00118-0

1. Introduction

In the past decade, many details on the topology and function of ion channels have been unveiled by using a variety of techniques including molecular biology, mutagenesis, patch-clamp recordings and their combinations. As bacterial membranes provide powerful systems for expressing channel proteins at a high level for the crystallization and X-ray analysis, the three-dimensional structures of channel proteins have begun to come into sight. For example, a crystal structure of a bacterial K^+ channel (KcsA) from *S. lividans* has been resolved at a resolution of 3.4 Å [1]. This structure is remarkably similar to the model inferred from years of electrophysiological studies on mutated and wild type K^+ channels [2]. This provides the first structural insights into possible mechanisms of ion selectivity and permeation for K^+ channels and fresh impetus to understand the permeation process of ions. We can surely expect that more and more three-dimensional structures of channel proteins will be resolved in the near future.

Nevertheless, without understanding how ions diffuse through the channel pore and how the channel protein interacts with water and ions, we cannot hope to understand the structure-function of channel proteins at the atomic level. At present, it is a challenge to biophysicists to understand how an ion channel functions from the microscopic point of view, even for a simple structured gramicidin channel [3]. Accordingly, constructing a minimalist channel-forming molecule is still a good strategy for the purpose of understanding how ions diffuse through a channel pore. Such strategy has been applied to several systems, such as the gramicidin-like channels [4–7], synthetic peptide channels [8–10], the porin channel [11] and the pore forming region of the K^+ channel [12].

It has been noticed that one of the common structural features among K^+ channels is that their internal vestibules are lined by predominantly hydrophobic amino acid side chains [13]. To get insight into the significance of the hydrophobic lining on the ion permeation, we performed molecular dynamics (MD) simulations of the ion permeation through a synthetic hydrophobic channel. The channel was constructed from a de novo synthetic cyclic octa-peptide, cyclo[-Ala-Aba(C_{16})-]$_4$ (AC164), consisting of four alternate L-alanine (Ala) and *N′*-acylated 3-aminobenzoic (Aba) moieties [14]. Despite its relatively simple structure, the AC164 channel shares basic properties with biological ion channels [15]. It displays a maximum conductance value of 9 pS when inserted into bilayer membranes. It excludes ions larger than radius of 3 Å, allowing for the passage of small monovalent cations while rejecting anions and divalent cations. The channel is supposed to be formed from a dimer of the molecule, in which the peptide ring forms the entrance of the channel and acyl chains line the channel pore. Owing to its relative simplicity and a pore having a common hydrophobic property with the K^+ channel, the simulation of the ion permeation through the AC164 channel should shed light on understanding the significance of the hydrophobic lining in the K^+ channel.

The simulations were an extension of our previous one in which the dynamic properties of intrapore water have been studied [10]. Therefore, the modified method is briefly described first. Then the potential energy profile of a Na^+ permeation through the AC164 channel is calculated by placing the Na^+ at different positions along the ion permeation path. Finally, the one-dimensional diffusion coefficient, $D(X)$, profile of the ion permeation along the channel axis is calculated. The obtained $D(X)$ profile shows that the ion can diffuse faster in the hydrophobic region than it can do in the bulk water and in a region lined with carbonyl oxygen atoms from the peptide ring. These results provide an insight, at the atomic level, into the significance of the hydrophobic lining of the K^+ channel. Some preliminary results have appeared elsewhere [16].

2. Materials and methods

2.1. Simulation system and MD simulations

Simulations were performed on a Silicon Graphics Indigo2 workstation using Insight II 95

and Discover 95 programs (Biosym/MSI, San Diego, CA, USA). CVFF forcefield parameters were used in all of the calculations. Molecules were built with the Builder program. Graphical displays were printed out from the Insight II molecular modeling system.

The CPK (space-filling) model and the simulation system of the channel are shown in Fig. 1a,b. Process of constructing channel system was the same as described earlier [10] except following modifications. A build-in pre-equilibrated water layer was selected to hydrate the channel. All water molecules are the SPC-type [17] with a partial charge on oxygen of -0.82 e (e is the elementary charge) and on hydrogen of 0.41 e. The initial channel system was constructed by replacing the water molecule at the center of the channel with a Na^+ ion (Fig. 1b). To mimic a condition of an ion in the bulk solution, more water molecules were added into the system. The whole system includes 7725 atoms: composed from 1714 cap water molecules, a model membrane

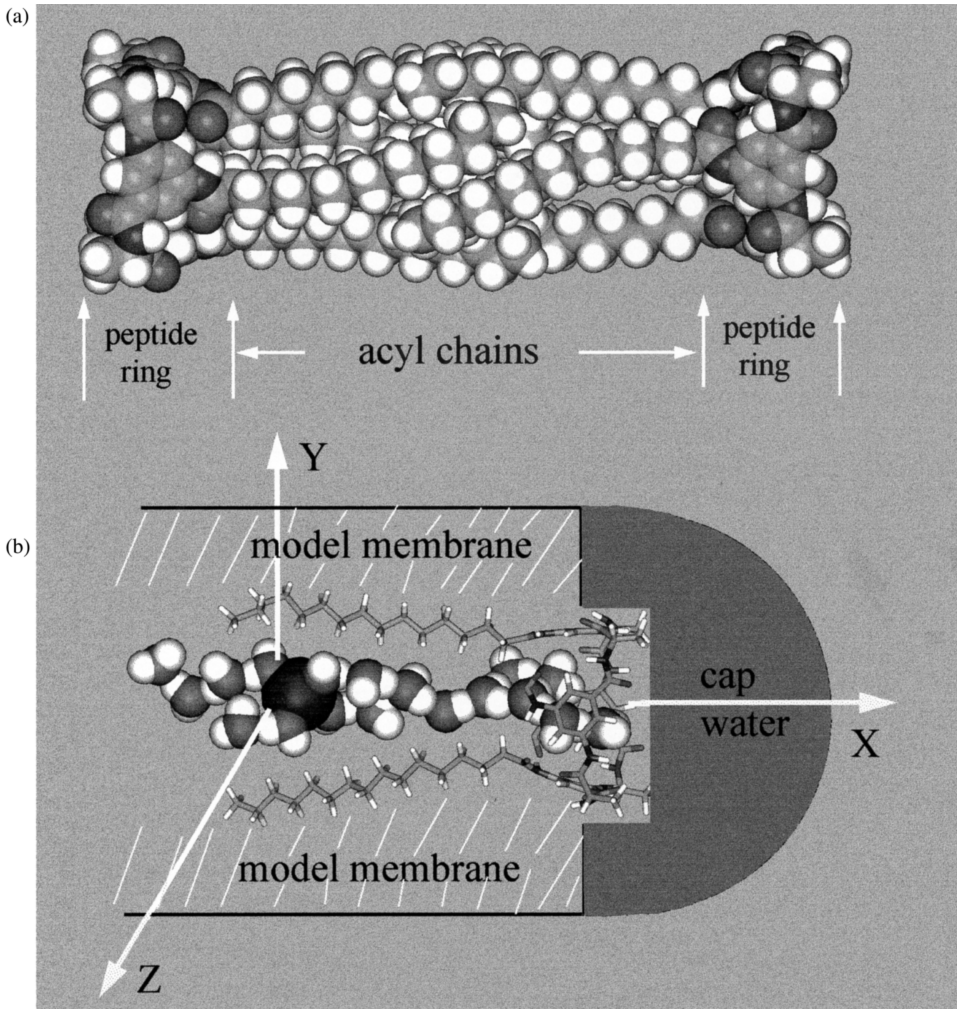

Fig. 1. Description of the simulation system: (a) is a side view of the AC164 channel; and (b) shows the simulation system. The origin of the coordinate system is located at the center of the channel. A snapshot of the Na^+ (dark ball) hydration configuration is shown by the CPK model. Two acyl chains of the channel shown by sticks were removed for clarity. The model membrane and cap water are composed of 640 $-CH_2-$ particles and 1714 water molecules. Only half of the system is shown on account for its symmetry.

formed from 640 $-CH_2-$ particles, 26 intrapore water molecules that was initially put into the channel, and a Na^+ ion. The group based electrostatic and van der Waals interactions were separately truncated smoothly at 15 and 10 Å along with a spline width of 1 Å and a buffer width of 0.5 Å. The channel axis is oriented along the X direction (Fig. 1b). The system was subjected to a four-stage energy minimization. The first two minimizations were used to refine the configuration of the outermost layer of the cap water and $-CH_2-$ particles formed from 663 cap water molecules and 370 $-CH_2-$ particles. During these two minimizations, the outermost layers were free to move while other parts of system were fixed. After this was done, the outermost layers were fixed in all of the following calculations to achieve the extended wall boundary condition [10]. The aim of the present study was to study the properties of ion permeation through the open channel. Therefore, a tether-type constraint was applied in the following two minimizations to keep the channel open and to avoid the acyl chains enter into the pore to block the ion permeation. To make the ion at an expected position, a tether-type restraint was also applied on the ion to restrain it at corresponding positions. These restraints were gradually reduced. After the maximal derivative of the final minimization became less than 0.1 kcal/mol, a two-stage MD simulation was carried out to equilibrate the system: (1) a 5-ps MD run was performed during which the tether-type restraint was further reduced; and (2) at the second equilibrium stage (10 ps), all the water molecules except the outermost layer of the cap water were set free to move. The Na^+ ion was also set free to move unless notified. All the $-CH_2-$ particles except the outermost layer were weakly tethered to mimic the hydrocarbon core of the lipid bilayer. Exactly the same condition was used in the production stage. As it was only weakly tethered, the channel always kept open and was able to fluctuate during the production stage of the MD run, a phenomenon which could be observed more clearly on animations of the MD runs. Simulation results of the production stage between a 100-ps and a 20-ps MD run were compared in central hydrophobic cavity and the acyl chain regions. No significant difference for total energy convergence, energetics and the diffusion coefficient of the ion was noticed. So the production stages of the simulations were performed for 20 ps, in which 200 average conformations were produced and saved for later analysis. All the data were obtained from analyzing those conformations. The same procedures from minimization to the production stage were repeated for each of 13 corresponding positions of the ion along the axis of the channel. In all of the MD simulations, Nosé dynamics at a time step of 0.5 fs were applied to avoid instability and inaccuracy of the system in the integration process of the MD run [10]. Therefore, even though each simulation is short (35 ps in total), the total time for 13 different positions of the ion is appreciable (455 ps in 910 000 steps for half-length of the channel). Same strategy of placing ion at various positions has been used by others [18,19] to calculate the energy profile.

2.2. Analysis

As described earlier [10], all the non-bonded interaction energies were calculated by using the Energy Analysis command of the Insight program, in which the cutoff radius was pre-set as 9.5 Å. To understand the energetics of the ion permeation through this hydrophobic channel, the total interaction energy (E_{Tol}) felt by the Na^+ was broken into its constituent terms as:

$$E_{\mathrm{Tol}} = E_{\mathrm{i\text{-}Pw}} + E_{i\text{-}\mathrm{Cw}} + E_{\mathrm{i\text{-}Ch}} + E_{\mathrm{i\text{-}Other}} \quad (1)$$

where $E_{\mathrm{i\text{-}Pw}}$, $E_{\mathrm{i\text{-}Cw}}$, $E_{\mathrm{i\text{-}Ch}}$, and $E_{\mathrm{i\text{-}Other}}$ represent the interaction energies of the ion with the intrapore water, the cap water, the channel and the rest components of the system, respectively. The interaction energy was not further decomposed to the electrostatic and van der Waals interaction as was previously done [10], because the electrostatic energy dominates the interaction energy and the van der Waals interaction plays little role in this channel. The dynamic change of the interaction energy around one position is reflected by calculating the average value of each energy terms

from the 200 conformations which were saved during the production stage of the MD run.

As the most important thing for an ion to cross the channel is its one-dimensional diffusion along the channel axis, i.e. X-axis, one-dimensional diffusion coefficient, $D(X)$, profile is used to demonstrate diffusion properties of the ion. The $D(X)$ is defined as:

$$D(X) = \lim_{t \to \infty} < [X(t) - X(0)]^2 > /2t. \quad (2)$$

The process of an ion permeation through the channel is inhomogeneous in nature. This is clearly demonstrated in Section 3.1 on the energetics of ion permeation. Therefore, during its displacement the ion wanders through regions with different diffusion constants. In practice, it seems not suitable to use $t \to \infty$ to describe the ion permeation process. Attempts to calculate the mean square displacement on a longer time scale lead to a growing uncertainty due to a worsening of sampling statistics when t becomes comparative with the simulation time. Due to these reasons, short time intervals of 2 ps were adopted to calculate the mean square displacement (MSD) of the ion. Such calculation has turned out to be a good way to compute the local diffusion constants of water permeation through a lipid membrane [20]. The value of $D(X)$ was calculated according to the least-square procedure (Marquardt–Levenberg algorithm) to fit the MSD curve using Eq. (2). To improve the fidelity of statistics, the time origin ($t = 0$) was shifted 0.05 ps one after another to obtain the $D(X)$ values at the time interval of 2 ps. These values were used to get the average $D(X)$ value of the ion (mean $\pm$ S.D.) at its corresponding average position during each of the 20 ps MD simulation. The $D(X)$ profile of the ion is constructed from these average values along the axis of the channel.

3. Results and discussions

3.1. Energetics of ion permeation

Even though the potential energy cannot be related directly to the rate of ion transition as the free energy can, it is still useful to correlate the interaction energy of ions with the structure of the channel [12,21,6]. Therefore, to understand the structure-function of the channel, we calculated the potential energy profile of the Na^+ ion permeation through the channel (Fig. 2a). Only half of the energy profile is represented on account of the symmetry of the channel. To simplify the description, we assume that the ion is diffusing from the cap region (right side) to the center (left side) of the channel.

The 'bulk solution' was approximated by placing the ion far beyond the channel entrance ($\sim$ 22 Å), where the ion is completely hydrated by the 'bulk water'. The total potential energy of the ion at this region is approximately -92 kcal/mol (Fig. 2a). In the peptide ring region (from $\sim$ 16 Å to 22 Å), the pore gives a negative energy (see ○, –·–·–· in Fig. 2a) to the ion mainly due to the carbonyl oxygen I (OI), II (OII) and III (OIII) atoms (Fig. 2c), each of which faces to the center of the pore (Fig. 2b) and has a negative charge of -0.38 e. At this region, the ion-cap water interaction (see Δ, ——— in Fig. 2a) goes toward zero, indicating that the ion is partly dehydrated. The cap water molecules still contributes a significant energy to stabilize the ion as shown in Fig. 2a, even after the ion moves into the channel. It is very difficult to do an MD calculation at a position of $\sim$ 15 Å without restraint, because during the equilibrium stage of the MD run the ion diffused away from the position as we expected and we got the ion at a different position in the production stage. To get rid of this difficulty, we applied a weak restraint that can just keep the ion at approximately $\sim$ 15 Å to get the interaction energy. Because the total ion–water interaction becomes weak, the energy profile begins to rise up at this position. An energy well, though shallow, is located between OII and OIII atoms ($\sim$ 17 Å), suggesting the location of a binding site for the ion permeation. This is supported by the $D(X)$ profile of the ion, in which the ion diffuses much slower, approximately $\sim$ 17 Å (Fig. 3a). It is worthy to mention that the location of the binding site is in agreement with the 'binding site' for water molecules [10] and our previous electro-

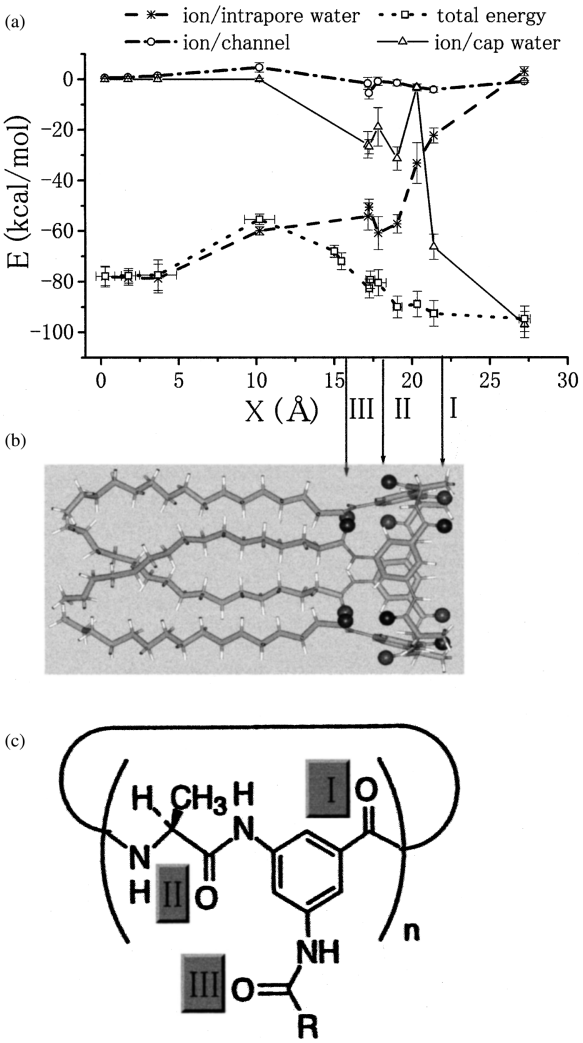

Fig. 2. Energetics of a Na^+ ion permeation through the channel. (a) Shows the potential energy profile of the ion and the interaction energy values contributed from each of other components of the system. Each symbol represents the mean ± S.D. of the interaction energy at corresponding position of the ion. (b) Shows the side view of the half channel. Arrows from right to left indicate oxygen I, II, III atoms in (c), which shows the chemical structure of the AC164 molecule ($n = 4$ and $R = C_{15}H_{31}$).

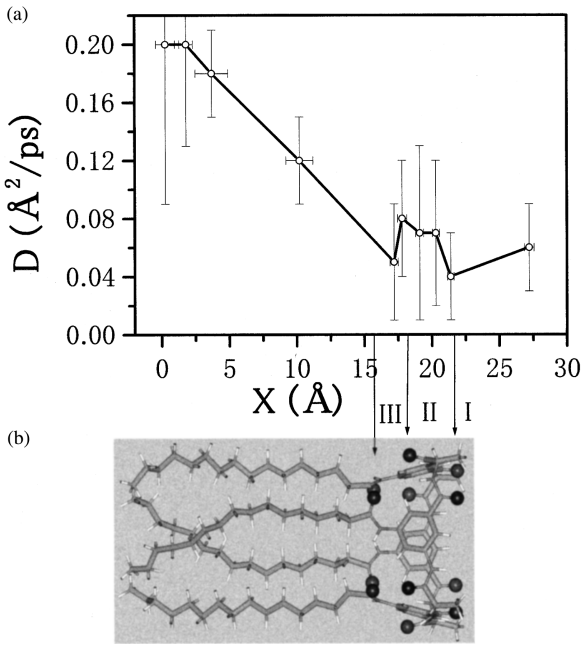

Fig. 3. (a) Shows the one-dimensional diffusion coefficient, $D(X)$, profile of the ion permeation through the channel. The symbols are the mean ± S.D. of the $D(X)$ value at corresponding position of the Na^+. (b) Shows the side view of the half channel. Arrows from right to left indicate the oxygen I, II and III atoms.

physiological data, which indicated that the binding site is located at the peptide ring [15]. When the ion moves further towards the center of the monomer (~ 10.5 Å), the interaction energy between the ion and the intrapore water molecules (see *, ------ in Fig. 2a) dominates the total interaction energy (see □, ... in Fig. 2a) of the ion. This means that the intrapore water is the main factor to stabilize the ion in the hydrophobic channel.

As the ion approaches the center of the channel, the total interaction energy goes down obviously. Unlike the peptide ring that is restrained by the rigid cyclic peptide bond [14], the acyl chains are much more flexible and can move in a wide range of space. This is consistent with the ESR (electron spin resonance) spectra of the spin-labeled hydrocarbon chain from both fatty acid and phosphatidylcholine, where a steadily increasing segmental motion down to the end of the acyl chain have been demonstrated [22]. Consequently, these acyl chains could expand out to create a big hydrophobic cavity (~ 9 Å in diameter). As a result, more water molecules could enter into the cavity to hydrate the ion and lower down the potential energy (Fig. 2a).

Thus, in the channel interior that is lined by

the pure hydrophobic acyl chains, the interaction energy is dominated by the interaction between water and ions. This result is different from that in the gramicidin A channel, where the channel also contributes to lowering the energy of the ion through its peptide backbone [3]. However, the energy difference between the well and the peak of the potential energy profile is comparable with the simulation result in the gramicidin channel [21] and in the pore region of the K^+ channel [12]. The potential energy well at the center of the AC164 channel is created by the intrapore water rather than from the pore. Thus, this well should not correspond to a binding site. An advantage of such a well located at the hydrophobic cavity is that the ion can stably stay there and diffuse fast at the same time (see below). This result might help us understand why there is a huge hydrophobic cavity (~ 10 Å in diameter) around the center of the K^+ channel [1].

3.2. Diffusion properties of the ion

Before going forward, let us recall the physical meaning of the ion diffusion coefficient (see also [23]). In aqueous solution, there is no intrinsic energy barrier for ion movement other than the local barriers of thermal fluctuations. Therefore, the diffusion coefficient describes a process in which the ion diffuses to any direction with equal chance. The externally applied gradient of electrochemical potential only produces a favorite direction for ion diffusion without any change of solvation structure of the diffusing ion. For ion diffusion in the channel, a diffusing ion will feel intrinsic electrochemical potential caused by the membrane-channel system and its hydration structure will be changed drastically. Therefore, the physical meaning of diffusion coefficient in ion permeation theory is not self-evident. For example, it reduces to an adjustable parameter, which can be obtained from fitting the experimental current-voltage relationship to the theory [24,25]. From a microscopic view, the diffusion process and $D(X)$ values of ion are always under the influence of the intrinsic electrochemical potential. Unlike its diffusion in the bulk solution, an ion diffusing in the channel will face to relatively large energy barriers. As a consequence, the diffusion of ion in the channel is in favor of diffusion down the barrier. Therefore, we must concern the direction of diffusion to describe the motion of ion in the channel. In the following, we calculate the $D(X)$ of the ion along the channel axis using Eq. (2), even though the forward and backward direction of ion diffusion cannot be distinguished there. The limitation of such a calculation will be discussed at the end of this section.

Diffusion properties of the Na^+ ion along its permeation pathway are summarized in Fig. 3, which shows the diffusion coefficient, $D(X)$, profile of the ion permeation through the channel. The value of $D(X)$ in the bulk solution was estimated to be ~ 0.06 Å^2/ps, which is close to the MD simulation results reported earlier [26–28]. Probably because the linear relation for $D(X) \sim t$ is only approximately fulfilled in confined systems [29], and due to the poor statistics associated with the limited simulation time and low ratio of the number of ions to the total number of molecules in the MD simulation [30], the S.D. value of the $D(X)$ is large.

Near the entrance of the channel four OI atoms from the carbonyl groups extend into the solution (Fig. 3b). As the ion approaches the channel entrance it encounters these OI atoms, i.e. the distance values between the ion and the OI atoms become small (Fig. 4). As the OI atoms face towards the center of the pore and bear negative charges, they trap the ion. As a result, the $D(X)$ of the ion is reduced relative to that of the bulk solution (Fig. 3a).

When the ion moves further into the channel, it interacts with the OII, then the OIII atoms. As the rigidity of the peptide ring keeps the OII atoms far from the channel axis, the interaction between the ion and the OII atoms is weaker, resulting in a slight increase in the $D(X)$. In contrast, as the average distance between the ion and the OIII atoms becomes smaller (Fig. 4), the ion moves slowly (curve 2 in Fig. 5), giving a small $D(X)$ value near the OIII atoms. This result is consistent with the conclusion from a detailed study of the trp-holorepressor that the diffusion coefficient of the surface water increases toward

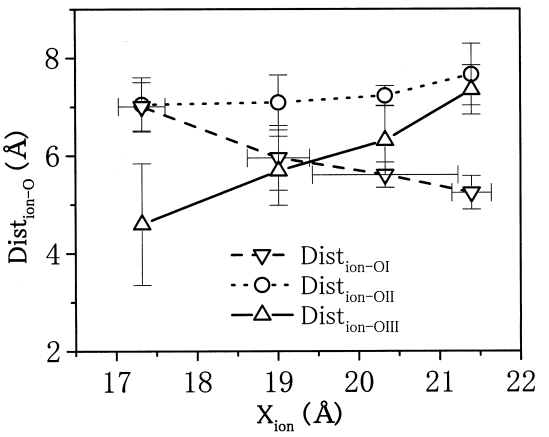

Fig. 4. The average distance between the Na^+ that is diffusing around the peptide ring and each oxygen (OI, OII and OIII) atoms on the peptide ring. The X-axis shows the positions of the Na^+ along the channel axis. At each position, only one point expresses the S.D. of X value of the Na^+ for clarity. The symbols are the mean $\pm$ S.D. of the average distance values ($Dist_{ion\text{-}O}$) between the Na^+ ion and the oxygen I, II, III atoms.

the bulk value as the distance of the water oxygen atom from the protein surface increases [31]. Therefore, the carbonyl oxygen atoms seem to play a role to slow down the diffusion of the ion inside the channel, even through the interaction between the ion and the carbonyl oxygen atoms is small (Fig. 2a). Comparing Fig. 4 and Fig. 3a, we can find that the closer the ion to the carbonyl oxygen atoms, the smaller the $D(X)$ of the ion. We can also see from Figs. 2 and 3a, that a well for both the $D(X)$ and the potential energy is located near the OIII atoms. This gives strong evidence that the binding site is near the OIII atoms.

When the ion approaches the center of the monomer ($\sim$10 Å), the $D(X)$ value becomes larger (Fig. 3). Comparing trajectory 2 and 3 in Fig. 5, we can see that the motion of the ion at the center of the monomer is much more violent than that in the peptide ring region, suggesting that the hydrophobic lining might play a role to accelerate the movement of ion. On the other hand, due to the potential energy barrier we can also see that the ion cannot diffuse equally in forward and backward directions (curve 3 in Fig. 5) as it can be in the cap and middle (curve 1 and 4 in Fig. 5) regions of the channel. Taken together, the large $D(X)$ value at this region might reflect a joint effect of a biased diffusion towards down the potential energy barrier (compare Fig. 2a and curve 3 in Fig. 5) and the accelerated motion of the ion. When the ion approaches the central region of the channel that spans from -5 to $+5$ Å, the $D(X)$ of the ion goes up further and becomes the largest at the center. Because there is no obvious energy barrier within this region, this result indicates that the diffusion of the ion is accelerated in the hydrophobic cavity rather than due to the joint effect of biased and accelerated diffusion like that in the region from $\sim$5 to 20 Å. Surprisingly, the central $D(X)$ value is much larger than that of the bulk solution. The hydrophobic property and the large size of the pore diameter at this region might explain this surprising result. In a pure hydrophobic environment there is no place for an ion binding, so the ion can diffuse smoothly and fast. The large size of the pore makes it possible that the ion can be stabilized by its surrounding water molecules (see the central well in Fig. 2a). Thus, the joint effect of these two factors lets the ion stably stay in the cavity and move fast at the same time. To the best of our knowledge, no study has been carried out to study the ion diffusion in a hydrophobic environment. However, we have found several lines of evidence to support an idea that the water molecule moves faster in hydrophobic cavities

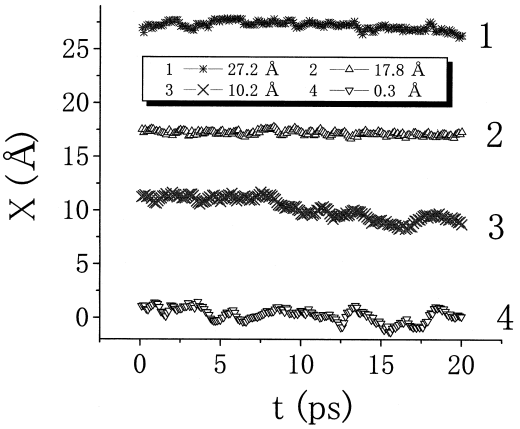

Fig. 5. Trajectories of the Na^+ ion at different average positions along the X-axis (indicated in inset).

than it does in hydrophilic environment. These might be taken as indirect evidence to support the accelerated motion of ion in the hydrophobic surroundings, because both ion and water possess the hydrophilic property. MD simulations of the water diffusion in the lipid bilayer membrane have indicated that the mobility of water is high in the center of the bilayer [20]. A similar result has been obtained from MD simulations on the water confined to a single smooth spherical cavity [29]. A disordered water molecule has been detected by the NMR but not by crystallography in a hydrophobic cavity of the human interleukin-1, implying that the mobility of water in the hydrophobic cavity is very high [32]. Besides, from their study of water in hydrophobic cavities, Buckle et al. [33] has indicated that water molecules may be present in the hydrophobic cavities but are too mobile to be detected by the crystallographic methods. On the contrary, we have noted an opposite phenomenon that the mobility of water molecules is reduced in a number of model channels [34–36]. One of the reasons for such contradictory observations might be that these channel pores are not so hydrophobic. Therefore, the backbone or polar side chains of the channel proteins might trap the water molecules and cause the reduction of water mobility.

Finally, assuming there is no interaction between ions, we will give a rough estimation of the ion flux in the AC164 channel based on the $D(X)$ profile (Fig. 3a) and the geometric parameters of the channel: length ($2L \sim 40$ Å) and radius (a $\geqq$ 3 Å) [15]. According to Levitt [37], the flux of monovalent cation can be expressed as:

$$J = [C_1 \exp(EF/RT) - C_2]/H, \tag{3.1}$$

$$x = X/L, (-20 \leqq X \leqq +20; \quad -1 \leqq x \leqq +1), \tag{3.2}$$

$$H = L\int_{-1}^{+1} [\exp(FV(x)/RT) /D(x)A(x)]\mathrm{d}x. \tag{3.3}$$

E is the voltage difference between side 1 and 2 of the bilayer membrane, $D(x)$ is the conventional ion diffusion coefficient, $A(x)$ is the area available for the ion, and $C(x)$ is the ion concentration. In the original definition [37], $V(x)$ is the total electrical potential, which is the sum of the applied external voltage and the intrinsic electrochemical potential of the channel. However, $V(x)$ should only be the applied external voltage here, because $D(X)$ values were calculated from the MD simulation of the ion that is already under the influence of the intrinsic potential of the whole system. As discussed, we cannot use $D(X)$ profile in Fig. 3 directly to calculate the ion flux due to the biased diffusion caused by the energy barrier, which is not considered in the definition of $D(X)$ in Eq. (2). To use the $D(X)$ profile for $D(x)$, we must consider the potential energy profile at the same time. From Fig. 2, we can see the potential energy goes up from $\sim$20 to 10 Å, so the large $D(X)$ value within this region should reflect a decelerated diffusion. From $\sim$10 to 5 Å, the potential energy goes down, indicating an accelerated diffusion. Combining the result in these two regions together, we might assume that part of the potential effect is canceled out. However, as the length and energy difference of peak-to-well from $\sim$20 to 10 Å is longer and higher than that from $\sim$10 to 5 Å, it is reasonable to set the lowest value of $D(X)$, i.e. 0.04 Å^2/ps, for the average $D(x)$ within the region from $\sim$20 to 5 Å. From $\sim$5 to -5 Å, the profile goes smoothly, so we may use the $D(X)$ value for $D(x)$ from Fig. 3. Based on these considerations, we may divide the ion permeation path into three regions for $D(x)$: (1) $D(x) = 0.04$ Å^2/ps for $-20 \leqq X \leqq -5$; (2) $D(x) = 0.2$ Å^2/ps for $-5 \leqq X \leqq +5$; and (3) $D(x) = 0.04$ Å^2/ps for $+5 \leqq X \leqq +20$. Furthermore, let $C_1 = C_2 = 100$ mM, $V(x) = (x+1)E/2$ ($E = 100$ mV), $A(x) = \pi a^2$ ($a = 3$ Å). Then, we obtain a flux value of $\sim 7.5 \times 10^6$ ions/s without using any adjustable parameters. This is equivalent to a conductance value of 12 pS at the above-assumed condition. This value is approximately the experimentally obtained maximum K^+ conductance ($\sim$9 pS), but two times as large as the maximum Na^+ conductance ($\sim$5 pS) of the channel [15], which might

reflect that the decelerated effect of the barrier was underestimated. This result reconfirms that the significant role of the hydrophobic cavity in KcsA K^+ channel [1] is to help the channel achieve a high throughput rate.

4. Conclusion and implications

Energetics and permeation properties of the Na^+ ion in the AC164 hydrophobic channel were investigated using MD simulations. The energy and $D(X)$ profiles of the ion permeation combined with the structure of the channel strongly suggest that the binding site of the Na^+ is located near oxygen III atoms. Due to the large hydrophobic cavity for water to access and the significant role of the water to stabilize the ion, an energy well instead of a peak is at the center of the channel. This result provides evidence to the suggestion that the hydrophobic cavity of the K^+ channel helps the diffusing ion to overcome the electrostatic destabilization resulting from the low dielectric bilayer by simply surrounding the ion with polarizable water [1]. Surprisingly, we found that the ion diffuses much faster in the central hydrophobic cavity than it does in the peptide ring region and the bulk solution. This result makes the significance of the hydrophobic lining of the K^+ channel more concrete by suggesting that the hydrophobic lining of the K^+ channel plays an active role to accelerate the movement of the diffusing ion. Accordingly, if an amino acid is mutated to a more hydrophobic residue on the inner vestibule of the K^+ channel, an increase in the channel conductance could be expected. It is very encouraging that we truly found a clue to support this idea. The single channel conductance values have increased when a threonine residue, T469, of the S6 segment of the Shaker K^+ channel was point mutated to more hydrophobic residues, such as alanine, isoleucine and valine [38].

Acknowledgements

We thank Dr D.P. Chen for critical reading the manuscript and valuable discussions. This work was supported by a grant from the future program of JSPS (to M. Sokabe). Z. Qi is a research associate of the future program of JSPS.

References

[1] D.A. Doyle, J.M. Cabral, R.A. Pfuetzner et al., Science 280 (1998) 69.
[2] S.R. Durell, H.R. Guy, Neuropharmacology 35 (1996) 761.
[3] B. Roux, M. Karplus, Annu. Rev. Biophys. Biomol. Struct. 23 (1994) 731.
[4] J. Åqvist, A. Warshel, Biophys. J. 56 (1989) 171.
[5] P.C. Jordan, Biophys. J. 58 (1990) 1133–1156.
[6] A. Pullman, Q. Rev, Biophys. 20 (1987) 173.
[7] B. Roux, B. Prod'hom, M. Karplus, Biophys. J. 68 (1995) 876.
[8] Q. Zhong, Q. Jiang, P.B. Moore, D.M. Newns, M.L. Klein, Biophys. J. 74 (1998) 3.
[9] D.P. Tieleman, M.S.P. Sansom, H.J.C. Berendsen, Biophys. J. 76 (1999) 40.
[10] Z. Qi, M. Sokabe, Biophys. Chem. 71 (1998) 35.
[11] A. Suenaga, Y. Komeiji, M. Uebayasi, T. Meguro, M. Saito, I. Yamato, Biosci. Rep. 18 (1998) 39.
[12] K.M. Ranatunga, I.D. Kerr, G.R. Smith, M.S.P. Sansom, Biochim. Biophys. Acta. 1370 (1998) 1.
[13] C.M. Armstrong, Science 280 (1998) 56.
[14] H. Ishida, K. Donowaki, Y. Inoue, Z. Qi, M. Sokabe, Chem. Lett. (1997) 953.
[15] Z. Qi, M. Sokabe, K. Donowaki, H. Ishida, Biophys. J. 76 (1999) 631.
[16] Z. Qi, M. Sokabe, Biophys. J. 76 (1999) A444.
[17] H.J.C Berendsen, J.P.M. Postma, W.F. van Gunsteren, J. Hermans, Jerusalem Symp. Quantum Chem. Biochem. 14 (1981) 331.
[18] G.R. Smith, M.S.P. Sansom, Biophys. J. 73 (1997) 1364.
[19] C. Etchebest, A. Pullman, FEBS 204 (1986) 261.
[20] S.J. Marrink, H.J.C. Berendsen, J. Phys. Chem. 98 (1994) 4155.
[21] M. Poxleitner, J. Seitz-Beywl, K. Heinzinger, Z. Naturforsch. 48c (1993) 654.
[22] Y.V.S. Rama Krishna, D. Marsh, Biochim. Biophys. Acta. 1024 (1990) 89.
[23] D.P. Chen, R.S. Eisenberg, J.W. Jerome, C.-W. Shu, Biophys. J. 69 (1995) 2304.
[24] D.P. Chen, L. Xu, A. Tripathy, G. Meissner, B. Eisenberg, Biophys. J. 76 (1999) 1346.
[25] S.-W. Chiu, J.A. Novotny, E. Jakobsson, Biophys. J. 64 (1993) 98.
[26] M. Berkowitz, W. Wan, J. Chem. Phys. 86 (1987) 376.
[27] S.H. Lee, J.C. Rasaiah, J. Chem. Phys. 101 (1994) 6964.
[28] A.P. Lyubartsev, A. Laaksonen, J. Phys. Chem. 100 (1996) 16410.
[29] L. Zhang, H.T. Davis, D.M. Kroll, J. Phys. Chem. 99 (1995) 2878.
[30] M. Canales, G. Sesé, J. Chem. Phys. 109 (1998) 6004.

[31] Y. Komeiji, M. Uebayasi, J. Someya, I. Yamato, Proteins Struct. Funct. Genet. 16 (1993) 268.
[32] J.A. Ernst, T.C. Robert, H-X. Zhou, A.M. Gronenborn, G.M. Clore, Science 267 (1995) 1813.
[33] A.M. Buckle, P. Cramer, A.R. Fersht, Biochemistry 35 (1996) 4298.
[34] J. Breed, R. Sankararamakrishnan, I.D. Kerr, M.S.P. Sansom, Biophys. J. 70 (1996) 1643.
[35] M.S.P. Sansom, I.D. Kerr, J. Breed, R. Sankararamakrishnan, Biophys. J. 70 (1996) 693.
[36] S.-W. Chiu, S. Subramaniam, E. Jakobsson, J.A. McCammon, Biophys. J. 56 (1989) 253.
[37] D.G. Levitt, Annu. Rev. Biophys. Chem. 15 (1986) 29.
[38] K.L. Choi, C. Mossman, J. Aubé, G. Yellen, Neuron 10 (1993) 533.